International Journal of Mechanics and Energy (IJME)
Vol. 1, Issue 2, 2013, ISSN: 2286-5845

Natural convection in a square cavity heated by an isothermal solid block

Basma SOUAYEH*, Nader BEN CHEIKH, Brahim BEN BEYA, Taieb LILI
Department of physics, 2092 El Manar 2, TUNISIA

Abstract: The present work deals with the prediction of a natural convection flow in a square cavity, partially heated by an obstacle placed at the bottom wall. The two transverse walls and the top wall of the cavity are supposed to be cold. The main parameter of numerical investigations is the Rayleigh number (engine convection) ranging from 10^3 to 10^5. Different configurations relative to cooling obstacle are presented and analyzed in the current study.

The simulations were conducted using a numerical approach based on the finite volume method and the projection method, which are implemented in a computer code in order to solve the Navier-Stokes equations.

Key words: natural convection, heat source, Rayleigh number, heat transfer, boundary conditions.

1. Introduction

Fluid mechanics allows to describe a wide variety of natural phenomena. It is of great importance in many fields such as aeronautics, chemistry, engineering or the environment. Many researchers investigated the fluid flow with heat transfer in environments incorporating isothermal obstacles or fins in confined cavities.

Among others, one can cite the work of Frederick [1] who studied natural convection in an inclined air-filled square enclosure with a diathermal partition for Rayleigh numbers between 10^3 and 10^5. The partition was attached to the cold wall and placed at its center. The partition relative length was 0.25 and 0.50 of that of the enclosure wall. Frederick [1] showed that the partition caused suppression of convection and that the heat transfer relative to that in an identical cavity without partition was reduced considerably. Tasnim and Collins [2] studied the effect of attaching a high conducting thin fin on the hot wall of an air-filled square cavity.

The effects of fin height and length, and the Rayleigh number on the heat transfer performance were investigated numerically. Tasnim and Collins [2] concluded that adding a fin on the hot wall increased the rate of heat transfer by about 31% compared with a wall without a fin. Bilgen [3] studied natural convection in differentially heated square cavities with a thin fin attached on the active wall. The Rayleigh number was varied from 10^4 to 10^9, dimensionless thin fin length from 0.10 to 0.90, dimensionless thin fin position from 0 to 0.90, dimensionless conductivity ratio of thin fin from 0 (perfectly insulating) to 60. Bilgen's [3] results showed that the Nusselt number is an increasing function of Rayleigh number, and a decreasing function of fin length and relative conductivity ratio. It was also found that the heat transfer might be suppressed up to 38% by choosing appropriate thermal and geometrical fin parameters.

*** Corresponding author:** Basma Souayeh
E-mail: basmasouayeh@gmail.com

Frederick and Valencia [4] investigated natural convection in a square enclosure with a fin placed on its hot wall and with perfectly conducting horizontal walls. The fin length and the solid to fluid thermal conductivity ratio were varied. For low values of the solid to fluid thermal conductivity ratio and the Rayleigh numbers in the range 10^4–10^5, reductions in heat transfer relative to the un-finned case were obtained. Frederick and Valencia [4] showed that this reduction is more pronounced when long fins are used. Ben-Nakhi and Chamkha [5] studied numerically two-dimensional, laminar, conjugate natural convection in a square enclosure with an inclined thin fin of arbitrary length. The authors showed that the thin fin inclination angle and length, and solid-to-fluid thermal conductivity ratio have significant effects on the local and average Nusselt numbers at the heated surfaces of the enclosure=fin system. They also reported that the presence of the inclined fin reduced the average Nusselt number at the heated surfaces in an unordered way. Other relevant papers related to the topic can also be consulted in references [6–13].

In the current investigation, a numerical study in terms of the problem of natural convection in cavities is carried out. The fluid is considered Newtonian and incompressible, we are mainly interested in two-dimensional cavities incorporating an obstacle on its hot wall. The side walls and the upper wall are maintained at a cold temperature T_c, while the remaining walls are kept adiabatic.

Several boundary conditions on different physical configurations or applications have been studied. We present in the first step the results for Rayleigh numbers ranging from 10^3 to 10^5. We present and analyze the flow structure and heat transfer through the active walls with the aid of plots of streamlines, isotherms and local Nusselt numbers.

2. Description of the model and numerical procedure

2.1 Problem formulation

The physical model considered in this work is shown in Figure 1, it's a square cavity or enclosure of side length H filled with a Newtonian incompressible fluid heated by an obstacle of length d and width e centrally fixed to the bottom wall. The vertical wall and the top wall are maintained at a cold temperature T_c<T_h.The remaining walls of the enclosure are kept insulated.

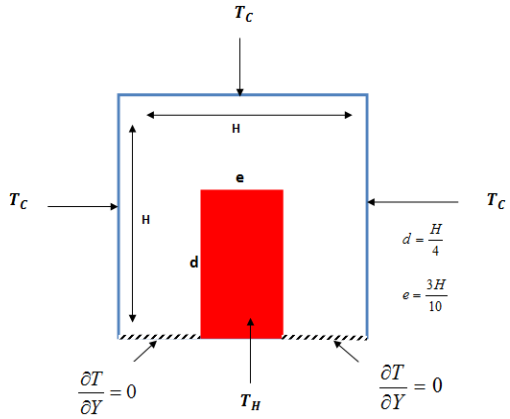

Fig. 1 Physical model and coordinates.

2.2 Numerical approach

The unsteady Navier–Stokes and energy equations are discretized by a second-order time stepping of finite difference type. A projection method [7] is used to solve the Navier–Stokes equations. An intermediate velocity is first computed and later updated for satisfaction of mass continuity. In the intermediate velocity field the old pressure is used. A Poisson equation, with the divergence of the intermediate velocity field as the source term, is then solved to obtain the pressure correction and the real velocity field.

A finite-volume method [8] is used to discretize the Navier–Stokes and energy equations. The advective terms are discretized using a QUICK third-order scheme [9] in the momentum equation and a second order central differencing one in the energy equation.

The discretized momentum and energy equations are resolved using the red and black successive over relaxation method RBSOR [10], while the Poisson pressure correction equation is solved using a full multigrid method (FMG) [11].

The convergence of the numerical results is established at each time step according to the following criterion:

$$\sqrt{\left(\sum_{i,j} X_{i,j}^{k} - \sum_{i,j} X_{i,j}^{k-1}\right)^2} \le 10^{-6}$$

where X stands for u, *v,* p, or θ and k is the iteration level.

The dimensionless governing equations for the present system can be expressed by the following unsteady, two-dimensional equations. In the light of the Boussinesq approximation the dimensionless equation are given by:

Continuity:

$$\frac{\partial u_i}{\partial x_i} = 0 \quad i = 1, 2 \quad (1)$$

Momentum:

$$\frac{\partial u_i}{\partial t} + \frac{\partial (u_i u_j)}{\partial x_j} = -\frac{\partial p}{\partial x_i} + \left(\frac{\Pr}{Ra}\right)^{\frac{1}{2}} \left(\frac{\partial^2 u_i}{\partial x_j \partial x_j}\right) + \theta \delta_{i2}$$

$i = 1, 2$ (2) $\quad \delta_{i2}$ is the Kronecker symbol.

Energy:

$$\frac{\partial \theta}{\partial t} + \frac{\partial (u_i \theta)}{\partial x_i} = \left(\frac{1}{Ra \Pr}\right)^{\frac{1}{2}} \frac{\partial^2 \theta}{\partial x_i \partial x_i} \quad i = 1, 2 \quad (3)$$

It is worth noting that equations were solved by an iterative method RBSOR coupled with a multigrid acceleration .

3. Results and discussion

3.1Code validation

The code was validated by Ben-Cheikh et al. [9]. In this work, the influence of the inclination of a cavity filled with an incompressible fluid containing an obstacle located on the bottom wall was studied. Table 1 summarizes some of the results obtained in ref. [12]. The authors showed (for moderate Rayleigh numbers) that a grid of 80×80 size was sufficient to obtain the results of the grid independence. For this reason, we used the code with the same grid size. In this investigation, boundary conditions have been modified in order to adapt the code to the present study.

3.2 Effect of Rayleigh number

Figure 2 shows the streamlines for wide ranges of Rayleigh number ($10^3 \le Ra \le 10^5$). It is noted that global flow pattern is described by two counter-rotating vortex and symmetrical with respect to the median plan. In addition, the increase of Rayleigh numbers tends to make the center of vortex upper with a slight inclination according to the midline.

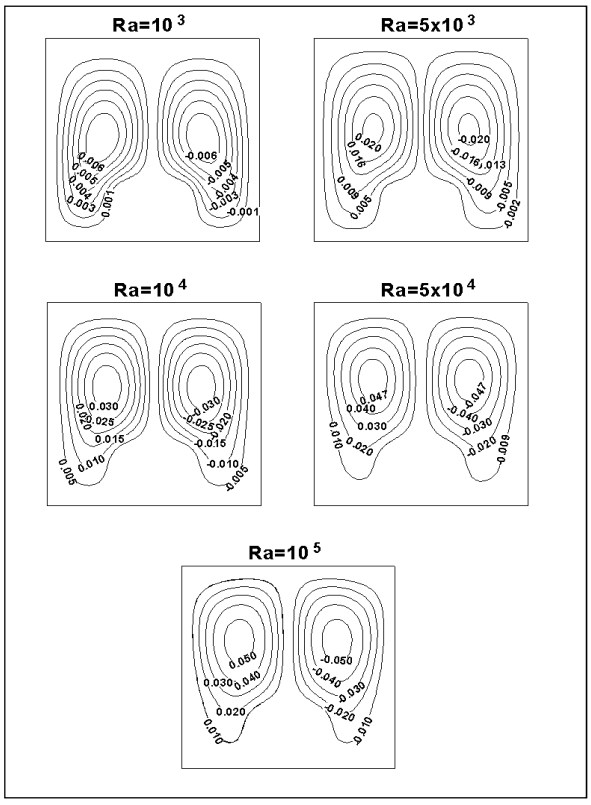

Fig.2 streamlines at the plan (x,y) for different Rayleigh numbers, Pr=0.71.

Figure 3 depicting the evolution of the temperature at the point (0.1, 0.7), clearly shows that the flow become unsteady by monotonously augmenting the number of Rayleigh until 5×10^5. According to this Rayleigh number value, a slight decrease is observed in the extreme values of the stream function. This decrease is explained by the fact that from Ra = $5x10^5$, a small areas of recirculation occurs at the horizontal wall of the obstacle. A zoom in this area detect the presence of these two secondary vortices (see Figure 4), which are at the origin of the transition to the unsteady state flow.

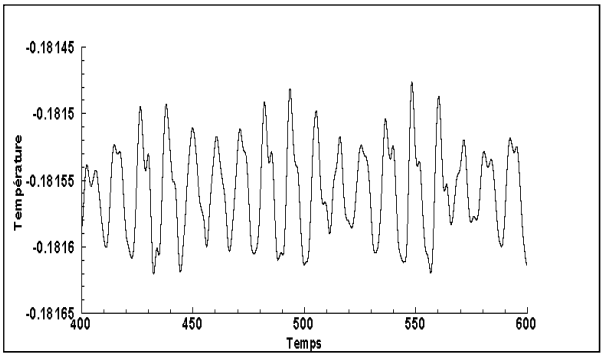

Fig. 3 Evolution of unsteady temperature versus time for Ra = 5××10^5 and Pr = 0.71.

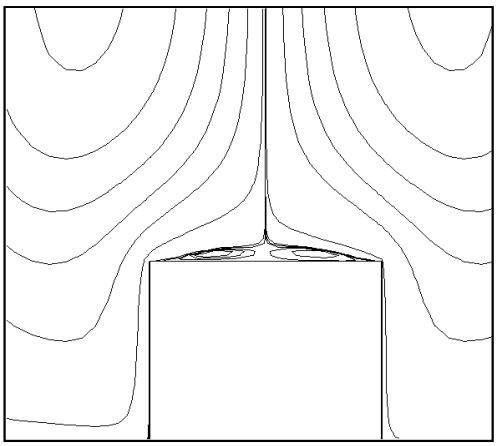

Fig. 4 Zoom of the streamlines at the horizontal wall of the obstacle for Ra = 5×10^5 and Pr = 0.71.

Profiles of the velocity component-v (x) at y = 0.5 for $10^3 \le Ra \le 10^5$ is plotted in Figure 5. In addition to the symmetry of the flow with respect to the center line x = 0.5, this figure shows that the rotational speed of the rotating vortex increases with the Rayleigh number.

We can also see that for a Rayleigh number in the range $10^3 \le Ra \le 10^5$, minimum values at the horizontal axis of the component v approaches to the center line x=0.5. Whereas, the opposite flow trend occurs when $Ra=10^5$.For low Rayleigh numbers $Ra=10^3$ and $Ra=5\times10^3$, the isotherms present almost concentric ellipsoid presenting a symmetrical structure with respect to the vertical plan passing through x = 1/2 (see Figure 6).

By further enhancing the Ra value, the deformation of the isotherms increases. In fact, thermal boundary layers become more and more tightened at the active walls and a net increase of thermal stratification is observed.

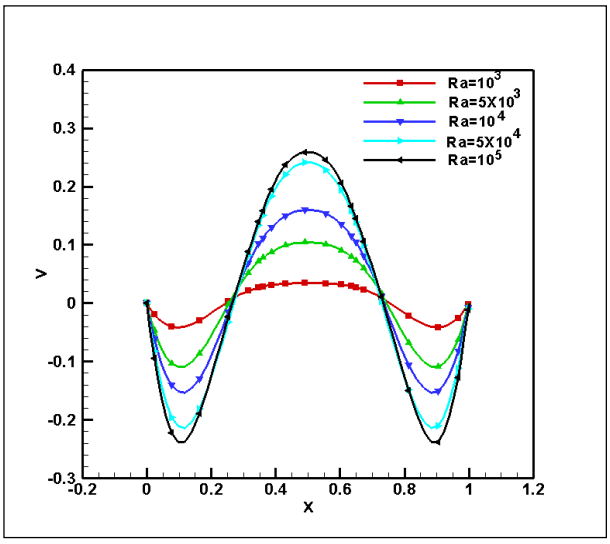

Fig. 5 Variation of the velocity profiles v versus x for different Rayleigh numbers at position y=0.5.

To study the average heat transfer at the vicinity of the active walls of the cavity, we computed the average Nusselt number at these walls (figure 7). The values obtained were used to establish a correlation in terms of the average Nusselt number and the Rayleigh number expressed as follows: $Nu_{moy} = 0.3084 \times Ra^{0.2702}$

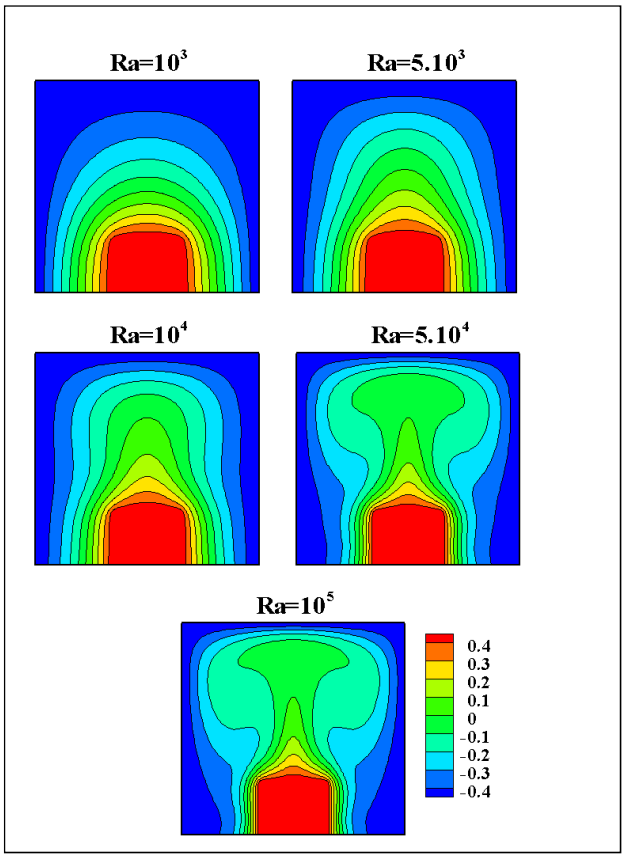

Fig. 6 Isotherms on different Rayleigh numbers in the plan(x, y).

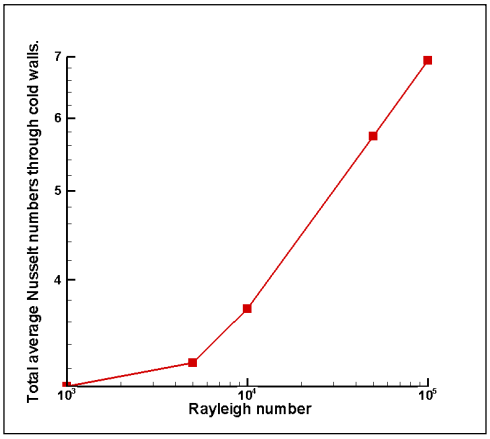

Fig. 7 Overall average Nusselt numbers computed at cold walls versus Rayleigh number for Pr=0.71.

3.3 Effect of the boundary conditions on the temperature

In order to study different ways of cooling the hot source, four configurations denoted by C2, C3, C4 and C5 are considered and shown schematically in figure 8.

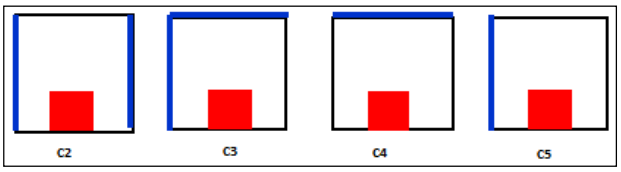

Fig. 8 Different cooling configurations

C2 and C3 configurations corresponding to the case where the hot obstacle is cooled by two walls, the remaining walls are supposed adiabatic, Configurations C4 and C5 are relative to a single wall cooling. When Ra = 10^3 and accordingly to configuration C2, we noted the appearance of two counterclockwise rotating vortexes symmetrically distributed with respect to the centerline. By slightly approaching the center of the cavity, the streamlines become tighter. Considering the configuration C3, one can notice the presence of a primary vortex turning counterclockwise and occupying the whole domain and the left part of the cavity. A clockwise rotating secondary vortex, with less volume seems to arise and occupy the right domain of the cavity. For configurations C4 and C5 the flow is almost the same as that observed for the case C2 C3. By increasing the number of Ra (Ra = 10^5), the general appearance of vortices remains unchanged.

Figures 8 and 9 reflect the isotherms for Ra = 10^3 and Ra = 10^5 relatively to the four configurations studied. For the low Rayleigh number value (Ra = 10^3) and far distant from the obstacle, the distance between the different iso-values of temperature remains almost constant meaning that the heat transfer is mainly due to conduction. Besides, the isotherms become more and more restricted near the hot and cold walls. We can also point out that these isotherms are more

deformed but remain in a good accordance with the structures of the flow vortex. Such phenomenon shows clearly the dominance of the mode of convective heat transfer for high Rayleigh numbers.

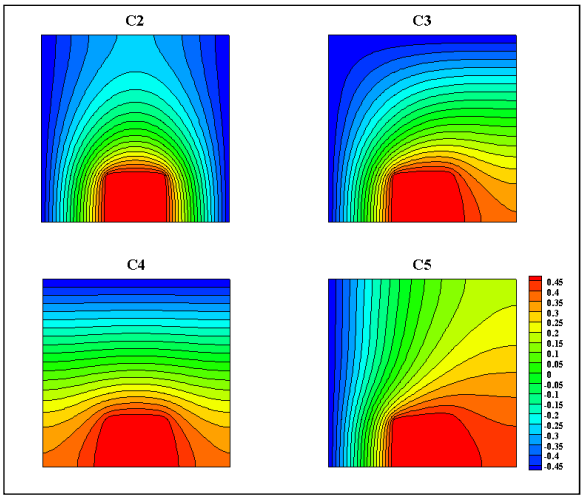

Fig. 9 Isotherms of different configurations for Ra = 10^3, Pr = 0.71.

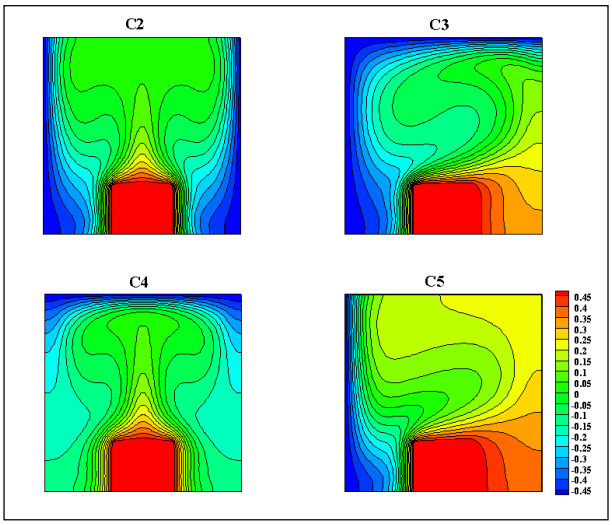

Fig. 10 Isotherms of different configurations for Ra = 10^5, Pr = 0.71.

Assuming that the general formula of the relative deviation is expressed as follows:

$$E_{\%} = \frac{\overline{Nu}_{\max} - \overline{Nu}_{\min}}{\overline{Nu}_{\min}} \times 100$$

Table 1 Comparision of Ben-Cheikh et al. [9] results and those of Frederic and Moraga[13]

	Nu(R_k=100)			Nu(R_k=1000)		
Ra	Ben-Cheikh et al.[9] study	[13]	Error(%)	Ben-Cheikh et al.[9] study	[13]	Error(%)
10^4	2.008	1.990	0.9	2.109	2.084	1.2
10^5	4.557	4.530	0.6	4.724	4.741	-0.4
10^6	9.293	9.312	-0.2	9.477	9.721	-2.5

Table 2 Variation of average Nusselt number values according to configurations C2 and C3 with respect to different Rayleigh and the corresponding relative errors.

Configurations	C2	C3	Relative deviations(%)
$\overline{Nu}\left(Ra=10^3\right)$	3.00	2.14	28.53
$\overline{Nu}\left(Ra=5\times10^3\right)$	3.20	2.39	25.28
$\overline{Nu}\left(Ra=10^4\right)$	3.63	2.88	20.51
$\overline{Nu}\left(Ra=5\times10^4\right)$	5.52	4.26	22.85

Table 3 Variation of average Nusselt number values according to configurations C4 and C5 with respect to different Rayleigh and the corresponding relative errors.

Configurations	C4	C5	Relative deviations (%)
$\overline{Nu}\left(Ra=10^3\right)$	1.17	1.80	34.46
$\overline{Nu}\left(Ra=5\times10^3\right)$	1.19	2.11	43.36
$\overline{Nu}\left(Ra=10^4\right)$	1.69	2.44	30.64
$\overline{Nu}\left(Ra=5\times10^4\right)$	3.55	3.55	0.10
$\overline{Nu}\left(Ra=10^5\right)$	4.42	4.19	5.29

The average Nusselt number was plotted as a function of Rayleigh number for all configurations. As expected, the Nusselt number increases with the Rayleigh for values less than Ra = 10^4 the Nusselt number remains weaker. Using the least squares method, correlation of the average Nusselt number and the Rayleigh number are proposed for C2, C3, C4 and C5, respectively ($5\times10^3 \le Ra \le 10^5$):

$$Nu_{moy} = 0.3820Ra^{0.2473}$$

$$Nu_{moy} = 0.2939Ra^{0.2471}$$

$$Nu_{moy} = 0.2175Ra^{0.2491}$$

$$Nu_{moy} = 0.1587Ra^{0.0597}$$

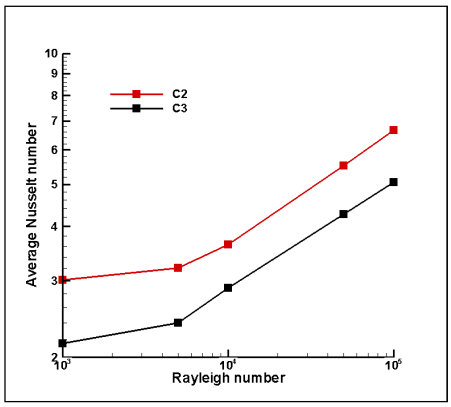

Fig.11 Evolution of average Nusselt number versus Rayleigh number for configurations 2 and 3, Pr = 0.71.

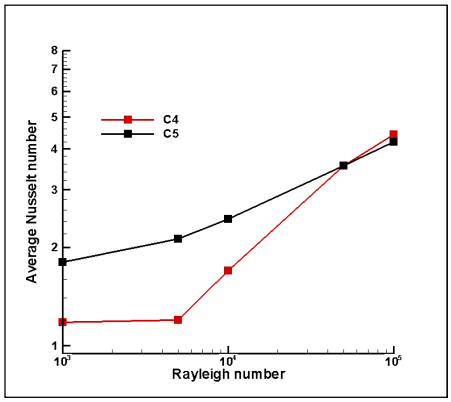

Fig.12 Evolution of average Nusselt number versus Rayleigh number for configurations 4 and 5, Pr = 0.71.

4. Conclusion

In the current study, we presented the results of the study of natural convection in a cavity with an obstacle on its hot wall for Rayleigh numbers ranging from 10^3 to 10^5. It should be noted that the flow remains steady for all Rayleigh numbers $Ra \leq 5.10^5$. This unsteady behavior is not analyzed in the current investigation but in another hand it will be extended for a three-dimensional case where unsteady phenomena is seen to be more apparent.

A correlation between the heat transfer medium through the active walls of the cavity and Rayleigh numbers could then be determined.

On another hand, the effect of different cooling configurations of the solid obstacle on the flow structure and thermal transfer is discussed and analyzed. It is found that, temperature boundary conditions strongly modify the internal flow pattern and the isotherms. Among the four studied configurations, those that correspond to maximum and minimum heat transfer rate were determined. Furthermore, correlations relatively to the four investigated configurations were proposed in terms of the average Nusselt number and Rayleigh number.

References

[1] R. L. Frederick, Natural Convection in an Inclined Square Enclosure with a Partition attached to its Cold Wall, Int. J. Heat Mass Transfer, vol. 32, pp. 87–94, 2008.

[2] S. H. Tasnim and M. R. Collins, Numerical Analysis of Heat Transfer in a Square Cavity with a Baffle on the Hot Wall, Int. Comm. Heat Mass Transfer, vol. 31, pp. 639–650, 2004.

[3] E. Bilgen, Natural Convection in Cavities with a Thin Fin on the Hot Wall, Int. J. Heat Mass Transfer, vol. 48, pp. 3493–3505, 2005.

[4] R. L. Frederick and A. Valencia, Heat Transfer in a Square Cavity with a Conducting partition on its Hot Wall, Int. Comm. Heat Mass Transfer, vol. 16, pp. 347–354, 1989.

[5] A. Ben-Nakhi and A. J. Chamkha, Conjugate Natural Convection in a Square enclosure with Inclined Thin Fin of Arbitrary Length, Int. J. Therm. Sciences, vol. 46, pp. 467–478, 2007.

[6] N. Kasayapanand, A Computational Fluid Dynamics Modeling of Natural Convection in Finned Enclosure under Electric Field, Appl. Thermal Eng., vol. 29, pp. 131–141, 2009.

[7] Y. Achdou, J.L. Guermond, Convergence analysis of a finite element projection/Lagrange–Galerkin method for the incompressible Navier–Stokes equations, SIAM J. Numer. Anal. 37 (2000) 799–826.

[8] S.V. Patankar, Numerical Heat Transfer and Fluid Flow, McGraw-Hill, New York, 1980.

[9] B.P. Leonard, A stable and accurate convective modelling procedure based on quadratic upstream interpolation, Comput. Meth. Appl. Mech. Eng. 19 (1979) 59–98.

[10] R. Barrett, etal.Templates for the Solution of Linear Systems: Building Blocks for Iterative Methods, SIAM, (1994).

[11] N. Ben Cheikh, Benchmark solution for time-dependent natural convection flows with an accelerated full-multigrid method, numerical heat transfer 52, 131-151(2007).

[12] N. Ben Cheikh, Ali J.Chamkha, Brahim Ben Beya, effect of inclination on heat transfer and fluid flow in a finned enclosure filled with a dielectric liquid, Num.Heat Trans.(A), 56, 286-300, 2009.

[13] R. L. Frederick and S. G. Moraga, Three-Dimensional Natural Convection in Finned Cubical Enclosures, Int. J. Heat and Fluid Flow, vol. 28, pp. 289–298, 2007.